NON-ORTHOGONAL TRANSMISSION UNDER FLEXIBLE ILLUMINATION PATTERNS FOR ADVANCED SATELLITE PAYLOADS

Tomás Ramírez[1], **Carlos Mosquera**[1], **and Nader Alagha**[2]

[1] *atlanTTic research center, University of Vigo, Vigo, Spain*
[2] *European Space Agency Technical Research Center (ESTEC) , Noordwijk, The Netherlands*

Keywords: Flexible payload, Non-Orthogonal transmissions, Rate-Splitting

Abstract

This works proposes a flexible illumination pattern with non-orthogonal transmissions, which reuse the same carrier frequency in different beams, to enhance the service quality for a region of interest within the satellite footprint. In particular, we assume an advanced satellite communication payload architecture, allowing for a flexible allocation of power and bandwidth across beams together with active antenna subsystems to relocate beams. To take a full advantage of the flexible payload capabilities, a non-orthogonal transmission scheme, known as Space-Time Rate Splitting, is utilized that only requires a minimum amount of channel state information to be known at the transmitter. Performance improvements, in terms of the minimum user throughput up to 50% with respect to single beam orthogonal transmission have been identified, as long as user terminals can apply a single-state successive interference cancellation. Lower gain values are observed when non-orthogonal transmission and conventional single user detection techniques are deployed at the receiver.

1. Introduction

New sophisticated payload designs have emerged in recent years to provide a flexible and dynamic allocation of the satellite resources, see, e.g., SES-15 [1] or Eutelsat Quantum [2]. In the latter case, up to eight beams can be created, with four beams per polarization, with flexibility in their locations and shapes. This allows the reconfiguration of the satellite in order to offer different services. These emerging satellite payloads with flexible resource allocation have paved the way for further studies of radio resource management (RRM) solutions. Along with new market opportunities, the flexible power, bandwidth and user beam positioning bring more technical challenges in designing practical resource allocation algorithms, as can be found in recent literature [3, 4]. The complexity of the resource management process increases even more if we include beamforming as an additional degree of freedom. In such a case, machine learning solutions are proposed to manage resource allocations in advance satellite payloads [5] [6].

In this work, we focus on flexible payload architectures and analyze how to leverage the flexible illumination of multiple beams to improve the spectral efficiency, hence the overall throughput when serving a particular region of interest (ROI) within the satellite user beam footprint. In our studies, we assume the beam size and the beam shape are pre-determined while the beam position (i.e., the center of the beam) is relocated to optimize the resource allocation. Let us note that the beam size is limited by the number of elements and the area of the antenna on board of the satellite.

It is shown that the system performance, measured in terms of the overall system throughput subject to a fair distribution among users, can be improved if the available on-board RF power is split among multiple beams to jointly serve users in the ROI. The idea is to surround a central beam with other supporting beams and share the available power and user frequency spectrum. In other words, the total transmitted RF power, and available user bandwidth remains the same, while frequency coloring scheme, frequency re-use, power allocation per beam and beams spacing are optimized to enhance the total system throughput, albeit in fairly distributed manner. The fairness is achieved in the proposed optimization scheme by maximizing the minimum rate offered to users within the ROI. As a benchmark scenario, we consider the system throughput when all users are served by single beam covering the ROI with an access to the total user bandwidth and available RF power.

We will analyze how the cooperation of multiple beams, optimally positioned to illuminate the ROI, can provide an improvement over the mere use of a single beam. We compare performance results of non-orthogonal transmissions among the beams, i.e., spectrum resources are reused, based on different frequency re-use schemes and user terminals capabilities. We focus on the gateway to user forward link, with only partial channel information available at the gateway in the form of the channel magnitudes or, equivalently, the signal-to-noise ratio of the receivers with respect to the different beams. For conventional receivers (with single user detection capability), similar approach to adjacent beam resource sharing [7] is used. In that case, the signal received from one beam is detected and other co-channel beams are treated as noise. Alternatively, we also consider more sophisticated receivers that can apply a single-stage successive interference cancellation.

We can take advantage of the advanced receivers with a rate-splitting technique for the mitigation of interference [8]. In a previous work by the authors [9], a rate-splitting technique operating with traditional satellite payloads was shown to provide a significant edge for the hot-spot scenario, a particular non-

uniform setting for which the power and bandwidth of all the surrounding beams are used to serve a central beam under a heavy traffic demand. We will extend this idea for advanced flexible payloads and illustrate how a multi-beam placement strategy with aggressive frequency reuse can result in a higher system throughput in the ROI while ensuring a fair distribution of data rates among users.

The rest of the paper is organized as follows. In Section 2, the satellite system model is introduced. Section 3 presents the illumination arrangement of the region of interest and frequency coloring scheme of the central and supporting beams. The design of the illumination pattern for the orthogonal and non-orthogonal transmissions is also detailed in Section 3, and the user rate allocation is described in Section 4. Afterwards, the illumination pattern is evaluated in Section 5. Finally, some conclusions are elaborated in Section 6.

2. System Model

We focus on the forward link of a GEO* multibeam satellite communication system which provides a regional coverage served by a small number of beams. An advanced satellite payload is assumed with flexible allocation of resources (i.e., on-board RF power and user spectrum) and adjustable beamforming. For simplicity, we assume a central beam with a fixed shape and beam size, as part of a group of steerable beams, all of them identical in beam size and beam shape. The beam spacing is assumed to be adjustable thanks to the deployment of an active antenna as part of the flexible payload. We consider this arrangement as non-orthogonal transmission since multiple users (in this case 7) are served simultaneously with a partially overlapping frequency plan that is determined based on the a frequency coloring pattern.

The motivation of the work is the provision of service of a "hot-spot" area with highly localized traffic demand, as the ROI within the satellite footprint. It is assumed that the size of this region of interest is comparable to the 3 dB contour of the central beam once this beam is properly pointed towards the ROI.

2.1 Region of Interest

The satellite payload can flexibly steer several beams towards the ROI. Inspired by previous results for serving areas with high-concentration of traffic demand [7, 9], we consider a system scenario in which only seven beams serve the ROI† as is depicted in Fig. 1a. A central beam (Beam 1), is established so that it mostly covers the ROI, the green area, and is surrounded by six supporting beams, the grey beams. Note that the adjustable beamforming using active antennas can deflect the supporting beams at a distance D which will be object of design; this deflection distance from the center of the ROI is normalized with respect to the 3 dB contour of the central beam (i.e., $D = 1$ corresponds to the 3 dB contour of beam 1). For the purpose of resource allocation, the ROI is divided into seven sectors, as it is sketched in Fig. 1b. Labels in Fig. 1b describe the association with the corresponding beams in Fig. 1a. Furthermore, the boundary of the inner sector (Sector 1) is determined based on a configurable threshold, G_{th}, with respect to the maximum signal strength of the central beam‡.

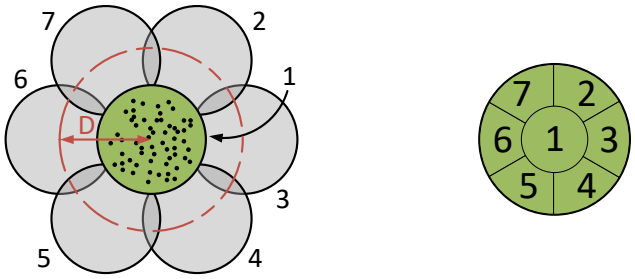

(a) (b)

Fig. 1 (a) The illumination beams pattern consists of a central beam and six surrounding beams to serve the region of interest. Black dots represent multiple users within the ROI to be served with the satellite resources. (b) The ROI is split into seven sectors served by the central beam and six surrounding beams.

2.2 Channel Model and Link Budget

As a first approximation, a channel model based on Bessel functions is used to characterize the radiation diagram of the satellite-user beams [4, 10]; the relative channel gain with respect to the maximum beam gain reads as

$$g_{ij} = \left(\frac{J_1(u_{ij})}{2 \cdot u_{ij}} + 36 \cdot \frac{J_3(u_{ij})}{u_{ij}^3} \right)^2 \tag{1}$$

with $u_{ij} \approx 2.07123 \cdot d_{ij}$, and d_{ij} the distance between the jth beam boresight and the user i, normalized by the 3 dB beam radius.

We assume that only partial channel information is available at the gateway, in the form of the channel magnitudes or, equivalently, the signal-to-noise ratios (SNRs). In particular, the SNR of the i-th user with respect to the j-th beam is expressed as

$$\gamma_{i,j} = g_{ij} \gamma^{ref} \tag{2}$$

where γ^{ref} is the SNR of a user located at the center of ROI served by a beam making use of all the available RF power P_T and user bandwidth W.

3. Illumination pattern coloring

The flexibility in the satellite payload allows to allocate overlapping carriers in different beams. Next, we present the two different frequency coloring for non-orthogonal transmissions. One is devised for traditional Single User Detection (SUD) receivers, whereas the other one takes advantage of the Successive Interference Cancellation (SIC) of advanced receivers. For

*We limit ourselves to the GEO scenario for modelling purposes. The presented ideas could also be applied to the non-GEO (NGEO) case.

†Performance analyses can be readily extended to other cases with different number of supporting beams or beam sizes.

‡The relative gain G_{th} is used for theoretical purposes. In an actual satellite system, it would be more practical to use instead signal to interference and noise (SINR) measurements at the receiver side which are reported back to the gateway.

benchmarking, we also consider a single beam focused on the ROI with the assignment of the whole transmission power and available frequency bandwidth.

3.1 Non-Orthogonal Transmission and SUD receivers

In [7], it has been shown that traditional single feed per beam non-flexible payloads, with Adjacent Beam Resource Sharing (ABRS), can serve the high traffic demand by employing the resources of neighbouring beams to increase the offered capacity to a hot-spot region[§]. For that purpose the ROI is split into seven sectors as presented in Fig. 2b, where a 3-color frequency pattern is assumed. Each label represents the assigned beam to that sector. This results in the illumination sketched in Fig. 2a. Thus, six sectors are served simultaneously with non-orthogonal (overlapping) carriers from the supporting beams, while the central sector is served by resources of the central beam. If we keep the same approach of resource sharing with a flexible payload and assume that the i-th user belongs to the central sector, the achievable user rate is given by

$$R_i = \alpha \cdot W \cdot \log_2\left(1 + \frac{\lambda}{\alpha} \cdot \gamma_{i,1}\right) \tag{3}$$

where α is the portion of bandwidth allocated to the central sector, and λ is the power allocated to the central beam.

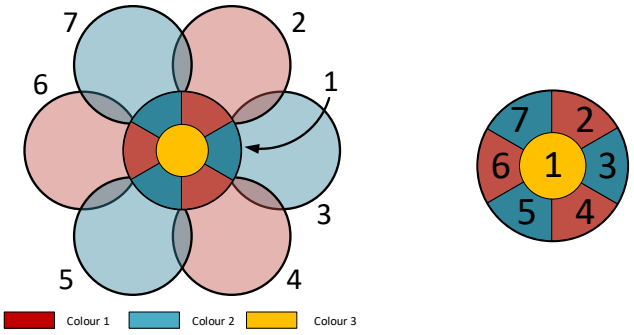

(a) (b)

Fig. 2 (a) Beams sectorization and coloring . Three different colors (red, blue and yellow) are used. (b) Illumination pattern.

In the outer sectors, the bandwidth is reused within two groups of three sectors each. If we assume that the j-th user operates at sector m, then the corresponding achievable rate can be obtained as

$$R_j = \beta_{\mathcal{S}} \cdot W \cdot \log_2\left(1 + \frac{\lambda_j \cdot \gamma_{j,m}/\beta_{\mathcal{S}}}{1 + \sum\limits_{\substack{p \neq m \\ m \in \mathcal{S}}} \lambda_{I(p)} \cdot \gamma_{j,p}/\beta_{\mathcal{S}}}\right) \tag{4}$$

where $\mathcal{S}$ is a set of sector indexes that employs the same color with bandwidth portion $\beta_{\mathcal{S}}$, $I(x)$ is a function that maps the beam index to the respective assigned user, and λ_j is the allocated power to the j-th user.

[§]The hot-spot scenario also fits into the system model that is described in Section 2.

3.2 Non-Orthogonal and SIC receivers

The joint application of rate-splitting and SIC at the receivers can exploit constructively the co-channel interference. With magnitude channel state information available at the transmitter, a rate-splitting strategy named Space-Time Rate-Splitting (STRS) can be applied [8]. Under the rate-splitting paradigm, different beams can transmit the superposition of a public and a private message under the same frequency to a group of users. The public message is encoded so that it can be successfully extracted by all user terminals belonging to the group, whereas private messages are only intended for one of the users within the group. In this work, we assume a unique public message which is suppressed by a single-stage SIC receiver.

In [9], it was shown how the rate-splitting approach can improve the spectral efficiency with respect to ABRS for Hot-spot scenarios in traditional payload systems. In that case, the frequency reuse after the beam sectorization can be more aggressive, as is shown in Fig 3(a). As opposed to the ABRS approach, the central beam reuses the bandwidth together with one of the groups of outer sectors. The rate-splitting scheme is able to exploit the resultant co-channel interference to increase the provided rates [8]. If we consider a flexible payload and its freedom in the resource allocation, we can go further in the frequency reuse and devise a sector coloring as that in Fig. 3(b), with both frequency colors reused by the central beam, and rate-splitting operating on the two different groups of four sectors.

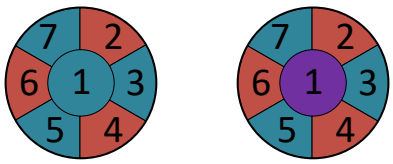

(a) (b)

Fig. 3 Beam sectorization and coloring for rate-splitting encoding. (a) Traditional payload. (b) Flexible payload. Two different colors (red and blue). Purple color represents full bandwidth.

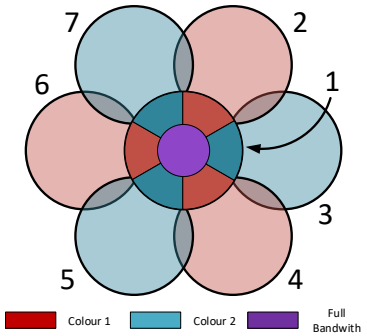

Fig. 4 Illumination pattern with rate-splitting encoding.

Let $\mathcal{R}$ be the indexes of a set of beams that apply the rate-splitting technique with bandwidth fraction $\beta_{\mathcal{R}}$, and $I(x)$ a function that maps the beam index to the respective assigned

user. If we define $\lambda^c_{k,m}$ and $\lambda^p_{k,m}$ as the fractions of total power allocated to the public and private messages, respectively, when the k-th user is served by the m-th beam, then the transmitted signal from beam m reads as

$$x_m = \sqrt{\lambda^c_{k,m} P_t} x^c_m + \sqrt{\lambda^p_{k,m} P_t} x^p_m \tag{5}$$

where x^c_m and x^p_m are the transmitted public and private messages by the beam m, respectively.

The different messages x^c_m convey a multicast public message which is decoded by all the users within the group. In the absence of phase information, space-time block codes (STBC) are the means to carry this public information; we assume the use of full rate STBC for analysis purposes. Then, the achievable rate of the public message can be expressed as

$$R^{\mathcal{R}}_c = \min_{I(m)} \left(R^c_{I(m)} \right) \ , \ m \in \mathcal{R} \tag{6}$$

$$R^c_{I(m)} = \beta_{\mathcal{R}} \cdot W \cdot \log_2 \left(1 + \frac{\sum_{h \in \mathcal{R}} \gamma_{I(m),h} \cdot \lambda^c_{I(h),h} / \beta_{\mathcal{R}}}{1 + \sum_{h \in \mathcal{R}} \gamma_{I(m),h} \cdot \lambda^p_{I(h),h} / \beta_{\mathcal{R}}} \right) \tag{7}$$

where (6) is set to ensure the decoding of the message by all the receivers in the group. On the other hand, the achievable rates of the private messages are obtained, after suppressing the public message, as

$$R^p_{k,m} = \beta_{\mathcal{R}} \cdot W \cdot \log_2 \left(1 + \frac{\gamma_{k,m} \cdot \lambda^p_{k,m} / \beta_{\mathcal{R}}}{1 + \sum_{\substack{h \in \mathcal{R} \\ h \neq k}} \gamma_{k,h} \cdot \lambda^p_{I(h),h} / \beta_{\mathcal{R}}} \right) \tag{8}$$

Since the information carried by the public message can be shared among the users in the group, the final rate of the k-th user when served by the m-th beam can be expressed as

$$R_k = a^{\mathcal{R}}_k \cdot R^{\mathcal{R}}_c + R^p_{k,m} \tag{9}$$

where $a^{\mathcal{R}}_k$ is the fraction of the public information that is allocated to the user k in the rate-splitting group $\mathcal{R}$.

3.3 Benchmark Scenario

As a benchmark, we consider the use of a single beam focused on the ROI making use of all the available resources (bandwidth and power). Thus, users are only served by the central beam (Beam 1) from Fig. 1a. With this, the achievable rate of the i-th user can be expressed as

$$R_i = \beta_i \cdot W \cdot \log_2 \left(1 + \frac{\lambda_i}{\beta_i} \cdot \gamma_{i,1} \right) \tag{10}$$

where β_i and λ_i are the fraction of carriers and power allocated to the i-th user.

4. Resource allocation

Once an illumination pattern is set, a resource allocation strategy needs to be devised to serve the users in the ROI. For the evaluation of techniques, we consider one user per sector, so that seven users compete for the resources.

In the case of the non-orthogonal transmissions, the ROI sectorization and the frequency coloring of the supporting beams create different user groups inside the ROI. The resource management process entails both the resource assignment to the groups, in terms of bandwidth and power, and the power allocation balancing inside each group. To simplify the optimization process, we assume that the portion of total power is equal to the portion of total bandwidth assigned to a user group. Furthermore, we consider two Quality of Service Criteria (QoS), namely, the maximization of the sum-rate, and the maximization of the minimum user rate. Next, we detail the optimization process for each considered technique.

4.1 Orthogonal: Single Beam

If we assume that the proportion of power is equal to the proportion of bandwidth, then the achievable user rates can be written as

$$R_n = \alpha_n \cdot W \cdot S_n = \alpha_n \cdot W \cdot \log_2 \left(1 + \gamma_{n,1} \right) \quad , n = 1, \dots 7 \tag{11}$$

with spectral efficiency $S_n = \log_2 \left(1 + \gamma_{n,1} \right)$. If we collect the values α_n in the vector $\boldsymbol{\alpha} = [\alpha_1 \cdots \alpha_K]$, the resource assignment is pursued to maximize the QoS function $f(R_n)$ with the following optimization problem:

$$\begin{aligned} \max_{\boldsymbol{\alpha}} \quad & f(R_n) \\ \text{subject to} \quad & \sum_{n=1}^{7} \alpha_n = 1 \end{aligned} \tag{12}$$

If we set the maximum rate as the optimization criteria, it can be easily deduced that the user with the highest SNR gets assigned all the resources:

$$\alpha_i = 1 \, , \quad i = \underset{n}{\operatorname{argmax}} \, S_n \quad , n = 1, \dots 7 \tag{13}$$

On the other hand, the optimal solution for the optimization of the minimum user rate can be easily obtained in closed form and it is given by

$$\alpha_n = \frac{\prod_{\substack{p=1 \\ p \neq n}}^{K} S_p}{\sum_{m=1}^{K} \prod_{\substack{p=1 \\ p \neq m}}^{K} S_p} \tag{14}$$

4.2 Non-Orthogonal: SIC receivers

If the allocated fractions of power and bandwidth are identical, then we can independently pursue the private versus public power balancing in rate-splitting within each rate-splitting group, as detailed in Appendix A. Following the frequency coloring and labeling in Figs. 3(b) and 4, we consider two different frequency colors A and B, and define the indexes set $\mathcal{R}_A = \{1, 2, 4, 6\}$ and $\mathcal{R}_B = \{1, 3, 5, 7\}$. With this user grouping, we optimize a given QoS criterion with the optimization process described in Appendix B. If the sum-rate is the optimization target, it is

clear that the group with the highest overall spectral efficiency after the optimization process receives all the available resources. On the other hand, the resource allocation has to be balanced to maximize the minimum user rate. Let $\text{Min}^{\mathcal{R}_A}$ and $\text{Min}^{\mathcal{R}_A}$ be the minimum spectral efficiency for the sets $\mathcal{R}_A$ and $\mathcal{R}_B$, respectively, after optimizing the power balance of the public and private messages. Again, the resource allocation for the optimization can be obtained with the closed form expression from (14):

$$\beta^{\mathcal{R}_A} = \frac{\text{Min}^{\mathcal{R}_B}}{\text{Min}^{\mathcal{R}_A} + \text{Min}^{\mathcal{R}_B}} \tag{15}$$

$$\beta^{\mathcal{R}_B} = \frac{\text{Min}^{\mathcal{R}_A}}{\text{Min}^{\mathcal{R}_A} + \text{Min}^{\mathcal{R}_B}} \tag{16}$$

where $\beta^{\mathcal{R}_A}$ and $\beta^{\mathcal{R}_B}$ are the portion of resources allocated to the groups formed by the sets $\mathcal{R}_A$ and $\mathcal{R}_B$, respectively.

4.3 Non-Orthogonal: SUD receivers

With ABRS, each beam transmits just one message intended to the user belonging to the corresponding sector. As in the previous section, we employ the numeration in Figs. 2b and 2a for the frequency coloring. A user from the central sector is served by the central beam (beam 1) with user rate:

$$R_1 = \alpha \cdot W \cdot S_1 = \alpha \cdot W \cdot \log_2(1 + \gamma_{1,1}) \tag{17}$$

where α is the portion of resources allocated to the central beam. Again, we are assuming equal fractions of power and bandwidth.

From Fig. 2b, the index sets $\mathcal{S}_A = \{2, 4, 6\}$ and $\mathcal{S}_B = \{3, 5, 7\}$ denote the user groups for the non-orthogonal transmissions. After the simplification detailed in Appendix C, we can decouple the power balancing within each beam from the resource allocation to each group.

The maximization of the sum-rate follows the same reasoning as before, so that all the resources are either allocated to the central beam or one of the groups with non-orthogonal transmissions. As to the maximization of the minimum user rate, the power balancing for the sets $\mathcal{S}_A$ and $\mathcal{S}_B$ is optimized by following Appendix D. Let $\text{Min}^{\mathcal{S}_A}$ and $\text{Min}^{\mathcal{S}_A}$ be the minimum spectral efficiency for the sets $\mathcal{S}_A$ and $\mathcal{S}_B$, respectively, after the power balancing in each group. Then, the optimal minimum user rate is obtained by solving the following minimax problem:

$$\begin{aligned} \max_{\alpha, \beta^{\mathcal{S}_A}, \beta^{\mathcal{S}_B}} \quad & \min(\alpha \cdot S_1, \beta^{\mathcal{S}_A} \cdot \text{Min}^{\mathcal{S}_A}, \beta^{\mathcal{S}_B} \cdot \text{Min}^{\mathcal{S}_B}) \\ \text{subject to} \quad & \alpha + \beta^{\mathcal{S}_A} + \beta^{\mathcal{S}_B} = 1 \end{aligned} \tag{18}$$

where $\beta^{\mathcal{S}_A}$ and $\beta^{\mathcal{S}_B}$ are the portion of resources allocated to the groups formed by the sets $\mathcal{S}_A$ and $\mathcal{S}_B$, respectively. From (14), the portion of the resources for the central user and two user groups are given by

$$\alpha = \frac{\text{Min}^{\mathcal{S}_A} \cdot \text{Min}^{\mathcal{S}_B}}{\nu} \tag{19}$$

$$\beta^{\mathcal{S}_A} = \frac{S_1 \cdot \text{Min}^{\mathcal{S}_B}}{\nu} \tag{20}$$

$$\beta^{\mathcal{S}_B} = \frac{S_1 \cdot \text{Min}^{\mathcal{S}_A}}{\nu} \tag{21}$$

$$\nu = S_1 \cdot \text{Min}^{\mathcal{S}_A} + S_1 \cdot \text{Min}^{\mathcal{S}_B} + \text{Min}^{\mathcal{S}_A} \cdot \text{Min}^{\mathcal{S}_B} \tag{22}$$

5. Numerical results

The performance of the considered technique has been tested for the different illumination patterns in Figs. 2a and 4. The simulations are parameterized by the power operation point of the system, through the reference SNR γ^{ref}, and the beam deflection D of the supporting beams. For each explored case, 400 Monte Carlo realizations have been run, with uniform distribution of users in each sector of the ROI. Note that perfect cancellation at the receive terminals when applying SIC is assumed for the STRS case. Furthermore, a practical application of the rate-splitting technique is also considered with only public information from the central beam, so that STBC is not required for encoding the public message. This solution can be considered a particular instance of NOMA (Non-Orthogonal Multiple Access). Table 1 summarizes the solutions under testing.

Table 1 Summary of the considered solutions.

Label	Technique	QoS	Transmissions
RS: SR	Rate-Splitting (STBC)	Sum-Rate	Non-Orthogonal
RS: Min	Rate-Splitting (STBC)	Minimum rate	Non-Orthogonal
RS-Prac: SR	Rate-Splitting (NOMA)	Sum-Rate	Non-Orthogonal
RS-Prac: Min	Rate-Splitting (NOMA)	Minimum rate	Non-Orthogonal
ABRS: SR	ABRS	Sum-Rate	Non-Orthogonal
ABRS: Min	ABRS	Minimum rate	Non-Orthogonal
Single: SR	Benchmark	Sum-Rate	Orthogonal
Single: Min	Benchmark	Minimum rate	Orthogonal

The threshold G_{th} sets the radius of the central sector which could be designed according to the user distribution inside the ROI. The effectiveness of the non-orthogonal solutions depends on how often the frequency can be reused for different users within the central beam. If a given sector is empty at a given time instant, the associated supporting beam is not turned on. In consequence, the threshold value G_{th} can be set to balance the traffic demand across sectors. One possible way of doing this, and without further considerations on the traffic demand per user, is to match the sector area and user density. If, for instance, we assume a uniform distribution of the users, the boundary of the central sector corresponds to a threshold $G_{th} = 0.365$ dB for a beam shape following the Bessel modeling. With this, the seven sectors have identical areas, and hence, an expected similar traffic demand.

The average aggregated spectral efficiency and minimum user spectral efficiency of the explored solutions are presented in Figs. 5 and 6 for an operation point $\gamma^{ref} = 20$ dB and different values of beam deflection D under the assumption of uniform user distribution. As a first observation, the practical application of rate-splitting without STBC presents a very close performance to rate-splitting with STBC. Therefore, we can avoid the STBC decoding at the receivers by operating with this simplified version, which amounts to NOMA, and that will be used hereafter. Furthermore, we can take advantage of the beamforming capabilities of the payload to steer the supporting beams and increase spectral efficiency. For the case under study,

$D = 2$ turns out to be the optimal beam deflection, ¶, with rate-splitting and ABRS providing 51% and 42% improvement, respectively, in terms of aggregated spectral efficiency over the single-beam case. Note that the minimum spectral efficiency in Fig. 6 is zero or close to zero, remarking that only one user or a user group is served with most of the available resources. Thus, overall throughout is obtained at the expense of a very unfair resource allocation.

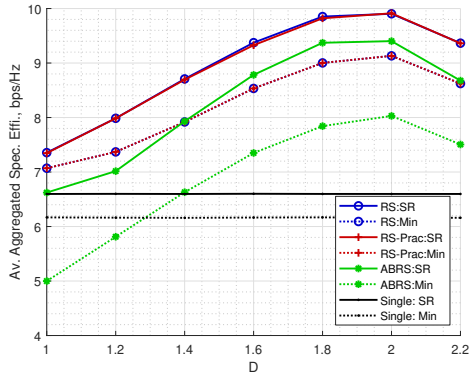

Fig. 5 Average aggregated spectral efficiency for different values of D. $\gamma^{ref} = 20$ dB. $G_{th} = 0.365$ dB.

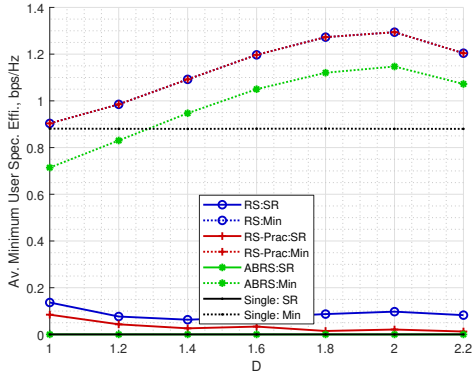

Fig. 6 Average minimum user spectral efficiency for different values of D. $\gamma^{ref} = 20$ dB, $G_{th} = 0.365$ dB.

Fairness is also looked at with the maximization of the minimum user spectral efficiency. Although both solutions with non-orthogonal transmissions are close for the maximization of the overall throughput, rate-splitting has an edge for providing a more fair allocation of the resources. The improvement with the rate-splitting technique is around 47%, and near 30% in the case of ABRS. If we assume a more unbalanced user distribution towards the boundaries of the central beam, we obtain the performances presented in Figs. 7 and 8. In this case, the user distribution requires $G_{th} = 1.5$ dB to obtain an equal volume of users per sector. Note that the improvement is higher than in the previous uniform user distribution case; the rate-splitting technique provides improvements around 67% and 72% in terms of aggregated and minimum user spectral efficiency, respectively.

¶The optimal beam deflection depends on the operation point.

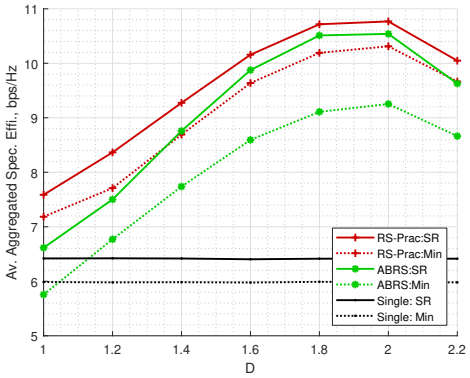

Fig. 7 Average aggregated spectral efficiency for different values of D. $\gamma^{ref} = 20$ dB, $G_{th} = 1.5$ dB.

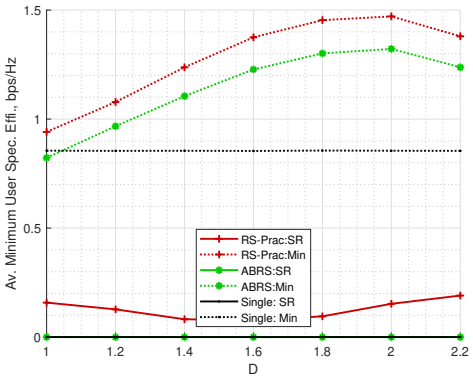

Fig. 8 Average minimum user spectral efficiency for different values of D. $\gamma^{ref} = 20$ dB, $G_{th} = 1.5$ dB.

The performance of the explored techniques does not only depend on the user distribution inside the ROI, but also on the operation point γ^{ref}, as it is related to the levels of co-channel interference among the supporting beams. For illustration purposes, we present the performance of the considered techniques in Figs. 5 and 6 for different operation points γ^{ref}, and fixed values of the inner radius, $G_{th} = 0.365$ dB, and beam deflection, $D = 2$. The rate-splitting provides higher gain as more transmission power is available, increasing the gap over ABRS and the single beam benchmark. Finally, let us remark that the performance of non-orthogonal schemes is highly dependent on the specific radiation pattern, due to the major role played by the co-channel interference. We leave for future studies the study of the beam shape to extract the best of the non-orthogonal transmissions.

6. Conclusions

This work has explored the application of illumination patterns with non-orthogonal transmissions to serve users inside a region of interest. Non-orthogonal transmissions are considered with multiple beams reusing the same portions of the spectrum, and two different solutions are presented in terms of receiver complexity with SUD and SIC receivers. The latter can take advantage of the co-channel interference thanks to the application

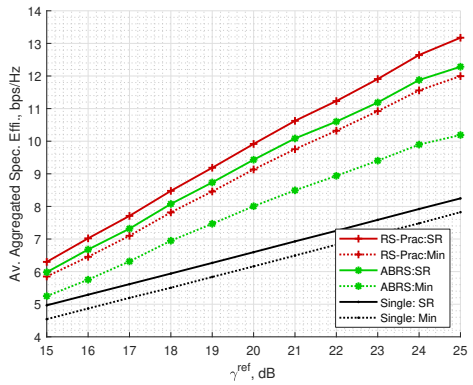

Fig. 9 Average aggregated spectral efficiency for different values of γ^{ref}. $G_{th} = 0.365$ dB, $D = 2$.

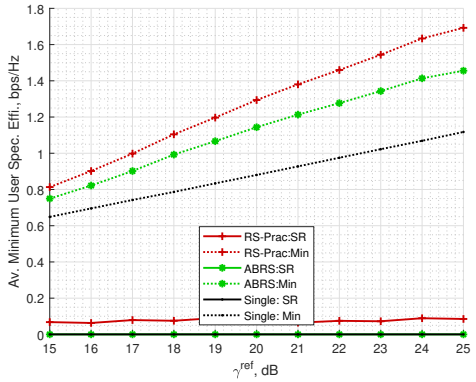

Fig. 10 Average minimum user spectral efficiency for different values of γ^{ref}. $G_{th} = 0.365$ dB, $D = 2$.

of a rate-splitting technique. The flexible allocation of power and bandwidth is addressed for two different QoS. From the results, the illumination pattern with non-orthogonal transmissions can significantly improve both overall aggregated spectral efficiency and minimum user spectral efficiency with improvements around 50 % for uniform distribution of the users inside the ROI. All in all, the power and bandwidth allocation to the different beams, along with the deflection of the external supporting beams, are tuned to optimize the performance boost with non-orthogonal transmissions for a given operation point. Future works could address the joint optimization of beam shaping and illumination pattern configuration to extract the best of the non-orthogonal transmissions.

Acknowledgment

Funded by the Agencia Estatal de Investigación (Spain) and the European Regional Development Fund (ERDF) through the project RODIN (PID2019-105717RB-C21). Also funded by Xunta de Galicia (Secretaria Xeral de Universidades) under a predoctoral scholarship (cofunded by the European Social Fund). The views of the authors of this paper do not reflect the views of the European Space Agency.

Appendix A
Achievable user rates with rate-splitting for equal portion of power and bandwidth

Section 3.2 details the achievable rates for a rate-splitting technique for a set of beam indexes $\mathcal{R}$. If we define $\chi_{\mathcal{R}}$ as the total power allocated to a group $\mathcal{R}$, we can redefine the power allocation of the private and public messages as

$$\lambda^{p}_{k,m} = \eta^{p}_{k,m} \cdot \chi_{\mathcal{R}} \tag{23}$$

$$\lambda^{c}_{k,m} = \eta^{c}_{k,m} \cdot \chi_{\mathcal{R}} \tag{24}$$

and simplify the rates for the rate-splitting from (7) and (8) as

$$\begin{aligned} R^{p}_{k,m} &= \beta_{\mathcal{R}} \cdot W \cdot \log_2 \left(1 + \frac{\eta^{p}_{k,m} \cdot \gamma_{k,m}}{1 + \sum\limits_{\substack{h \in \mathcal{R} \\ h \neq k}} \eta^{p}_{I(h),h} \cdot \gamma_{k,h}} \right) \\ &= \beta_{\mathcal{R}} \cdot W \cdot {S_k}^{p,m} \end{aligned} \tag{25}$$

$$\begin{aligned} R^{c}_{I(m)} &= \beta_{\mathcal{R}} \cdot W \cdot \log_2 \left(1 + \frac{\sum\limits_{h \in \mathcal{R}} \eta^{c}_{I(h),h} \cdot \gamma_{I(m),h}}{1 + \sum\limits_{h \in \mathcal{R}} \eta^{p}_{I(h),h} \cdot \gamma_{I(m),h}} \right) \\ &= \beta_{\mathcal{R}} \cdot W \cdot S^{\mathcal{R}}_{c} \end{aligned} \tag{26}$$

Then, we can rewrite (9) as

$$R_k = a^{\mathcal{R}}_{k} \cdot R^{\mathcal{R}}_{c} + R^{p}_{k,m} \tag{27}$$

$$= \beta_{\mathcal{R}} \cdot W \cdot \left(a^{\mathcal{R}}_{k} \cdot S^{\mathcal{R}}_{c} + {S_k}^{p,m} \right) \tag{28}$$

$$= \beta_{\mathcal{R}} \cdot W \cdot S_k \tag{29}$$

and pursue the optimization of the power allocation independently of the resource assignment to the groups.

Appendix B
Optimization process for the power allocation in rate-splitting

Here, we detail the rate optimization for the rate-splitting technique from Section 3.2 with the rate simplification from Appendix A. If we have a rate splitting group $\mathcal{R}$ with N users, N optimization problems need to be solved, one for each user setting the minimum rate of the public message in (26). From this relation, we have that R_c=$R^{c}_{I(m)}$ if, for $m = \{1, 2 ..., N\}$ and $m \neq k$,

$$\theta_{mk} + \sum_{h \in \mathcal{R}} \eta^{p}_{I(h),h} \left(\frac{\gamma_{I(m),h}}{\alpha_{I(m)}} - \frac{\gamma_{I(k),h}}{\alpha_{I(k)}} \right) \geq 0 \tag{30}$$

with

$$\alpha_{I(m)} = 1 + \sum_{h \in \mathcal{R}} \gamma_{I(m),h}\,, \quad \theta_{mk} = \frac{1}{\alpha_{I(m)}} - \frac{1}{\alpha_{I(k)}} \tag{31}$$

With this, the N non-convex sub-problems P_i which need to be solved to maximize the QoS are expressed as

$$
\begin{aligned}
(P_i) \quad \underset{\eta^p_{I(h),h},\eta^c_{I(h),h}}{\operatorname{argmax}} \quad & \min_k S_k \\
\text{subject to} \quad & \theta_{mk} + \sum_{h\in\mathcal{R}} \eta^p_{I(h),h} \left(\frac{\gamma_{I(m),h}}{\alpha_{I(m)}} - \frac{\gamma_{I(k),h}}{\alpha_{I(k)}} \right) \geq 0 \\
& k = 1, 2, ..., N, m \neq k \\
& \sum_{h\in\mathcal{R}} \eta^p_{I(h),h} + \sum_{h\in\mathcal{R}} \eta^c_{I(h),h} \leq 1 \\
& 0 \leq \eta^p_{I(h),h}, \eta^c_{I(h),h} \leq 1, \, , \quad h \in \mathcal{R}
\end{aligned}
\tag{32}
$$

where S_k is the spectral efficiency of the user k from Appendix A. The different maximization sub-problems can be pursued by applying a sequential quadratic programming method [11]. The optimal solution will be the best among the obtained solutions.

Appendix C
Achievable user rates with ABRS for equal portion of power and bandwidth

Section 3.1 details the achievable rates with the ABRS technique for a set of beam indexes $\mathcal{S}$. If we define $\chi_{\mathcal{S}}$ as the total power allocated to the colour of the group $\mathcal{S}$, we can express the allocated power to the j-th user who operates at sector m as $\lambda_j = \eta_j \cdot \chi_{\mathcal{S}}$ and rewrite the rates, assuming that the power fraction is equal to the allocated bandwidth fraction, as

$$
R_j = \beta_{\mathcal{S}} \cdot W \cdot \log_2 \left(1 + \frac{\eta_j \cdot \gamma_{j,m}}{1 + \sum\limits_{\substack{p\neq m \\ m\in\mathcal{S}}} \eta^{I(p)} \cdot \gamma_{j,p}} \right) \tag{33}
$$

Thus, we can pursue the optimization of the power allocation independently of the resource assignment to the groups.

Appendix D
Optimization process for the power allocation in ABRS

Here, we detail the rate optimization for the rate-splitting technique from Section 3.1 with the rate simplification from Appendix C. If S_j is the spectral efficiency of the user j from Appendix C, the following minimax optimization problem maximizes the considered QoS:

$$
\begin{aligned}
\underset{\eta_j}{\operatorname{argmax}} \quad & \min_j S_j \\
\text{subject to} \quad & \sum_{p\in\mathcal{S}} \eta_{I(p)} \leq 1 \\
& 0 \leq \eta_{I(p)} \leq 1 \, , \quad p \in \mathcal{S}
\end{aligned}
\tag{34}
$$

where S_j is the spectral efficiency of the user j from Appendix C. The maximization problem can be pursued by applying a sequential quadratic programming method [11].

References

[1] SES. Flexible satellite. [Online]. Available: https://www.ses.com/press-release/ses-and-thales-unveil-next-generation-capabilities-onboard-ses-17

[2] EUTELSAT. Flexible satellite. [Online]. Available: https://www.eutelsat.com/fr/satellites/futurs-satellites/Eutelsat-Quantum.html

[3] G. Cocco, T. De Cola, M. Angelone, Z. Katona, and S. Erl, "Radio Resource Management Optimization of Flexible Satellite Payloads for DVB-S2 Systems," *IEEE Trans. Broadcast.*, vol. 64, no. 2, pp. 266–280, 2018.

[4] A. Paris, I. Del Portillo, B. Cameron, and E. Crawley, "A Genetic Algorithm for Joint Power and Bandwidth Allocation in Multibeam Satellite Systems," in *2019 IEEE Aerospace Conference*. IEEE, 2019, pp. 1–15.

[5] W. Bailer, M. Winter, J. Ebert, J. Flavio, and K. Plimon, "expectation-maximization for scheduling problems in satellite communication," in *2020 25th International Conference on Pattern Recognition (ICPR)*.

[6] F. G. Ortiz-Gomez, D. Tarchi, R. Martínez, A. Vanelli-Coralli, M. A. Salas-Natera, and S. Landeros-Ayala, "Cooperative multi-agent deep reinforcement learning for resource management in full flexible vhts systems," *IEEE Transactions on Cognitive Communications and Networking*, pp. 1–1, 2021.

[7] N. Alagha, "'Adjacent Beams Resource Sharing to Serve Hot Spots'," in *35th AIAA International Communications Satellite Systems Conference, International Communications Satellite Systems Conferences (ICSSC)*, Oct 2017.

[8] C. Mosquera, N. Noels, T. Ramírez, M. Caus, and A. Pastore, "Space-Time Rate Splitting for the MISO BC with Magnitude CSIT," *IEEE Transactions on Communications*, pp. 1–1, 2021.

[9] T. Ramírez, C. Mosquera, M. Caus, A. Pastore, N. Alagha, and N. Noels, "Adjacent beams resource sharing to serve hot spots: A rate-splitting approach," in *36th AIAA International Communications Satellite Systems Conference*, Niagara Falls, Canada, Oct 2018.

[10] C. Caini, G. E. Corazza, G. Falciasecca, M. Ruggieri, and F. Vatalaro, "A spectrum- and power-efficient EHF mobile satellite system to be integrated with terrestrial cellular systems," *IEEE Journal on Selected Areas in Communications*, vol. 10, no. 8, pp. 1315–1325, 1992.

[11] J. Nocedal and S. J. Wright, *Numerical Optimization*, 2nd ed. New York, NY, USA: Springer, 2006.